1396 *Biochemistry* **2010,** *49,* 1396–1403
DOI: 10.1021/bi9021318

BIOCHEMISTRY
including biophysical chemistry & molecular biology
*Article*

# Inactivation of *Lactobacillus leichmannii* Ribonucleotide Reductase by 2′,2′-Difluoro-2′-deoxycytidine 5′-Triphosphate: Adenosylcobalamin Destruction and Formation of a Nucleotide-Based Radical[†]

Gregory J. S. Lohman,[‡] Gary J. Gerfen,[∥] and JoAnne Stubbe*[,‡,§]

[‡]*Department of Chemistry, and* [§]*Department of Biology, Massachusetts Institute of Technology, Cambridge, Massachusetts 02139, and* [∥]*Albert Einstein College of Medicine, Jack and Pearl Resnick Campus, 1300 Morris Park Avenue, Ullmann Building, Room 225, Bronx, New York 10461*

*Received December 11, 2009; Revised Manuscript Received January 18, 2010*

ABSTRACT: Ribonucleotide reductase (RNR, 76 kDa) from *Lactobacillus leichmannii* is a class II RNR that requires adenosylcobalamin (AdoCbl) as a cofactor. It catalyzes the conversion of nucleoside triphosphates to deoxynucleotides and is 100% inactivated by 1 equiv of 2′,2′-difluoro-2′-deoxycytidine 5′-triphosphate ($F_2$CTP) in < 2 min. Sephadex G-50 chromatography of the inactivation reaction mixture for 2 min revealed that 0.47 equiv of a sugar moiety is covalently bound to RNR and 0.25 equiv of a cobalt(III) corrin is tightly associated, likely through a covalent interaction with $C_{419}$ (Co−S) in the active site of RNR [Lohman, G. J. S., and Stubbe, J. (2010) *Biochemistry 49*, DOI: 10.1021/bi902132u]. After 1 h, a similar experiment revealed 0.45 equiv of the Co−S adduct associated with the protein. Thus, at least two pathways are associated with RNR inactivation: one associated with alkylation by the sugar of $F_2$CTP and the second with AdoCbl destruction. To determine the fate of [1′-$^3$H]$F_2$CTP in the latter pathway, the reaction mixture at 2 min was reduced with $NaBH_4$ ($NaB^2H_4$) and the protein separated from the small molecules using a centrifugation device. The small molecules were dephosphorylated and analyzed by HPLC to reveal 0.25 equiv of a stereoisomer of cytidine, characterized by mass spectrometry and NMR spectroscopy, indicating the trapped nucleotide had lost both of its fluorides and gained an oxygen. High-field ENDOR studies with [1′-$^2$H]$F_2$CTP from the reaction quenched at 30 s revealed a radical that is nucleotide-based. The relationship between this radical and the trapped cytidine analogue provides insight into the nonalkylative pathway for RNR inactivation relative to the alkylative pathway.

Ribonucleotide reductases (RNRs)[1] catalyze the conversion of nucleotides to deoxynucleotides, providing the monomeric precursors required for DNA replication and repair (*1*−*5*). Class I and class II RNRs are stoichiometrically inactivated by the 5′-di- and triphosphate forms of 2′-deoxy-2′,2′-difluorocytidine (Gemzar or $F_2$C), a drug presently used clinically in the treatment of advanced pancreatic cancer and non-small cell lung carcinoma (*6*−*11*). The *Lactobacillus leichmannii* ribonucleoside triphosphate reductase (RTPR), a monomer with a molecular mass of 76 kDa, is the paradigm for adenosylcobalamin (AdoCbl) requiring RNRs, although recent genomic analyses have revealed that the dimeric class II enzymes, exemplified by the recently crystallized *Thermotoga maritima* RTPR, are much more prevalent than the monomeric forms (*12*−*15*). In the following paper (*16*), we reported the synthesis of [1′-$^3$H]-, [1′-$^2$H]-, and [5-$^3$H]$F_2$CTP and showed that 1 equiv of [1′-$^3$H]$F_2$CTP resulted in 90% inhibition of the enzyme within 30 s, with 0.47 equiv of $^3$H covalently attached to the enzyme (*16*). Our earlier studies demonstrated that during this inactivation, on a 30 min time scale, RTPR became covalently labeled with the corrin ring of AdoCbl through $C_{419}$, one of the active site cysteines providing reducing equivalents to generate dNTPs (*17*). In this work, we describe our efforts to examine the fate of AdoCbl immediately subsequent to enzyme inactivation and the fate of the remaining $F_2$CTP that is not covalently attached to the enzyme. As with many mechanism-based inhibitors of RNRs, multiple modes of inhibition are observed (*1*, *18*). A model for accommodating our observations described in this paper in relationship to the observations in the following paper (*16*) is presented (Scheme 1).

## MATERIALS AND METHODS

*Quantification and Characterization of Cobalamin, Cytosine, and Nucleotide Products Generated from RTPR Inactivated by $F_2$CTP.* The inactivation mixture in a final volume of 1250 μL contained prereduced RTPR (50 μM), dATP (500 μM), AdoCbl (50 μM), HEPES (25 mM, pH 7.5), EDTA (4 mM), and $MgCl_2$ (1 mM). After addition of AdoCbl, all aliquots were handled under red light and wrapped with foil. The inactivation was initiated by addition of either [1′-$^3$H]$F_2$CTP (SA of 1985 cpm/nmol) or [5-$^3$H]$F_2$CTP (SA of 1350 cpm/nmol) to a final concentration of 50 μM. An aliquot was assayed for activity as described in the following paper (*16*). The inactivation was allowed to proceed for either 2 min or 1 h at 37 °C. An aliquot (100 μL) was removed

[†]Funding for this study was provided in part by National Institutes of Health Grant GM-29595.

*To whom correspondence should be addressed. Telephone: (617) 253-1814. Fax: (617) 258-7247. E-mail: stubbe@mit.edu.

[1]Abbreviations: RNR, ribonucleotide reductase; Gemzar or $F_2$C, 2′,2′-difluoro-2′-deoxycytidine; $F_2$CDP, 2′,2′-difluoro-2′-deoxycytidine 5′-diphosphate; $F_2$CTP, 2′,2′-difluoro-2′-deoxycytidine 5′-triphosphate; RTPR, ribonucleoside triphosphate reductase; AdoCbl, adenosylcobalamin; SA, specific activity; HOCbl, hydroxycobalamin; *ara*-C, arabinocytidine; RFQ, rapid freeze quench; GSCbl, glutathionine cobalamin; Y•, tyrosyl radical; α, ribonucleotide reductase large subunit.

 Published on Web 01/20/2010 

Scheme 1: Proposed Model for the Mechanism of Inactivation of RTPR by $F_2$CTP by the Nonalkylative and Alkylative Pathways

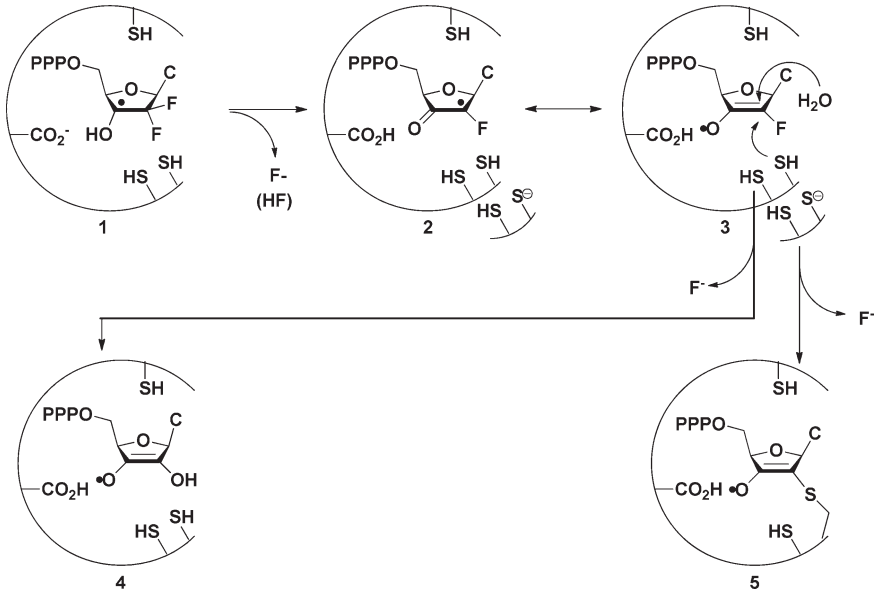


after 2 min and after 1 h and quenched by filtration through a YM-30 membrane at 4 °C, and the nucleotides were dephosphorylated with alkaline phosphatase and analyzed by HPLC. An aliquot of 1000 $\mu$L after 2 min and 1 h was loaded on a Sephadex G-50 column (1 cm × 20 cm, 20 mL) wrapped in foil, run at 4 °C under dim red light. The column was equilibrated in and eluted with 25 mM HEPES (pH 7.5), 4 mM EDTA, and 1 mM $MgCl_2$, and 1 mL fractions were collected. Each fraction was assayed for $A_{260}$ and $A_{280}$, and for radioactivity (100 $\mu$L). Aliquots (750 $\mu$L) from the protein-containing fractions were combined, and the UV−vis spectrum was recorded. These fractions were then lyophilized to dryness (excluding light). Aliquots (750 $\mu$L) from the small molecule fractions (pooled when $A_{260} > A_{280}$) were combined and lyophilized to dryness (excluding light). These samples were dissolved in 500 $\mu$L of water, and the UV−vis spectra were recorded. The spectrometer baseline was determined via lyophilization of an equal volume of buffer identical to that used in the experimental samples, which was redissolved in 500 $\mu$L of water. The visible spectra of protein-associated cobalamin products were quantified by comparison to a standard of glutathionine cobalamin (GSCbl) (*19*). The corrin species not associated with the protein were deconvoluted through linear combinations of the spectra of AdoCbl and HOCbl standards in proportions of AdoCbl to HOCbl ranging from 1:0 to 0:1 in 0.05 equiv increments. The samples were scaled to match the $A_{525}$ of the experimental sample and subtracted.

*Characterization of the Major Nucleoside Product(s) Isolated from a $NaBH_4$-Quenched RTPR/$F_2$CTP Inactivation Mixture*. The reaction mixture in a final volume of 2 mL contained RTPR (125 $\mu$M), dATP (500 $\mu$M), AdoCbl (125 $\mu$M), $F_2$CTP (125 $\mu$M), HEPES (25 mM, pH 7.5), EDTA (4 mM), and $MgCl_2$ (1 mM). The inactivation was quenched at 2 min with 500 $\mu$L of 250 mM $NaBH_4$ in 500 mM Tris (pH 8.5) in a 4.0 mL Falcon tube and the mixture incubated for 5 min at 37 °C. The $NaBH_4$ solution was prepared via combination of solid $NaBH_4$ with the buffer immediately before use. Vigorous foaming occurred during the inactivation. The solution was then filtered through a YM-30 membrane for 15 min at 14000*g* and 4 °C, and the flow-through was treated with 200 units of alkaline phosphatase for 2 h at 37 °C, followed by filtration through a second YM-30 membrane. The sample was acidified by addition of glacial acetic acid, and the resulting mixture was lyophilized to dryness to hydrolyze borate esters. The residue was then taken up in 1 mL of 10 mM $NH_4OAc$ and purified on an Altech Adsorbosphere Nucleotide Nucleoside C-18 column (250 mm × 4.6 mm) using a 2 mL injection loop with elution at a flow rate of 1 mL/min. The solvent system for elution was composed of buffer A [10 mM $NH_4OAc$ (pH 6.8)] and buffer B (100% methanol). The products were eluted with 100% A for 10 min followed by a linear gradient to 40% B over 25 min and then to 100% B over 5 min. Under these conditions, the standards eluted as follows (compound, retention time): cytosine, 5.7 min; uracil, 7.9 min; cytidine (C), 12.6 min; arabinocytidine (*ara*-C), 17.4 min; deoxycytidine (dC), 19.0 min; and $F_2$C, 23.2 min. Diode array detection of the eluent allowed identification of cytosine-containing nucleosides between 17 and 22 min. These fractions were pooled, and the recovery of cytosine-containing nucleosides was determined to be ~60 nmol based on $A_{270}$. This material was lyophilized to dryness, taken up in 1 mM $NH_4OAc$, and repurified using the same elution program, substituting 1 mM $NH_4OAc$ (pH 6.8) for buffer A and retaining buffer B (100% MeOH). The major cytosine-containing material eluted at 16.2 min and was collected (~35 nmol), lyophilized, and rechromatographed a third time. The final recovery of nucleoside was typically 8−12 nmol: $^1$H NMR (500 MHz, $D_2O$) $\delta$ 7.71 (d, $J$ = 7.5 Hz, 1H, H6), 5.99 (d, $J$ = 6.1 Hz, 1H, H1′), 5.85 (d, $J$ = 7.5 Hz, 1H, H5), 4.41 (dd, $J$ = 5.6 Hz, 1H, H2′), 4.24 (dd, $J$ = 4.3, 4.9 Hz, 1H, H3′), 4.02 (m, 1H, H4′), 3.80 (dd, $J$ = 4.0, 12 Hz, 1H, H5′), 3.75 (dd, $J$ = 7.0, 12 Hz, 1H, H5″); ESI-MS ($C_9H_{13}N_3O_5$) $m/z$ ($M + Na^+$) calcd 266.0747, observed 266.0743, ($M + H^+$) calcd 244.0928, observed 244.0921.

*Characterization of the Major Nucleoside Product Isolated from a $NaBD_4$-Quenched RTPR/$F_2$CTP Inactivation Mixture*. A reaction was run in a manner identical to that described above, except that $NaBD_4$ was substituted for $NaBH_4$. The final recovery of the trapped nucleotide after three purifications was ~5−8 nmol: $^1$H NMR (500 MHz, $D_2O$) $\delta$ 7.71 (d, $J$ = 7.5 Hz, 1H, H6), 5.98 (s, 1H, H1′), 5.84 (d, $J$ = 7.5 Hz, 1H, H5), 4.01 (dd, $J$ = 4.0, 7.1 Hz, 1H, H4′), 3.80 (dd, $J$ = 4.0, 12 Hz, 1H, H5′), 3.75 (dd, $J$ = 7.0, 12 Hz, 1H, H5″).

*High-Frequency EPR/ENDOR Spectroscopy*. Samples for D-band (130 GHz) EPR analysis were prepared from a reaction mixture that in a final volume of 50 $\mu$L contained RTPR (300 $\mu$M), dATP (1 mM), AdoCbl (450 $\mu$M), $F_2$CTP (unlabeled or labeled with 1′-$^2$H or 3′-$^2$H) (300 $\mu$M), TR (20 $\mu$M), TRR (0.5 $\mu$M), NADPH (1 mM), and HEPES (25 mM, pH 7.5). The dATP and reductants were mixed, followed by addition of RTPR. The AdoCbl was then added and mixed in low light, and the inhibition was initiated by the addition of $F_2$CTP or [1′-$^2$H]-$F_2$CTP. The reaction mixture was drawn up into the D-band EPR sample tube (outside diameter of 0.55 mm, inside diameter of 0.4 mm) mounted in the plastic tip of a pipet-man and then the reaction quenched in isopentane cooled with liquid nitrogen. The reaction time was 30 s. The tubes were mounted in the D-band probe under liquid nitrogen, and pulsed EPR/ENDOR spectra were recorded on a spectrometer described elsewhere (*20*, *21*) using parameters listed in the figure legend of Figure 4. The field for D-band EPR spectra was calibrated using $Mn^{2+}$ doped in MgO (*22*).

## RESULTS

*Fate of AdoCbl during the Inactivation of RTPR by $F_2$CTP*. To gain a better understanding of the partitioning between the inactivation mechanism associated with covalent modification by a sugar moiety derived from $F_2$CTP (*16*) and the one associated with covalent modification of $C_{419}$ by the corrin, the fate of AdoCbl was investigated. Inactivation studies were conducted with a 1:1:1 AdoCbl:RTPR:$F_2$CTP ratio, and the protein and small molecules were separated by Sephadex G-50 chromatography and analyzed at 2 min and 1 h. The small molecules and protein were analyzed for corrin by UV−vis spectroscopy either before or after concentration. Despite the detection by stopped flow spectroscopic methods on the millisecond time scale of cob(II)alamin (0.7 equiv/RTPR) and by the rapid freeze quench (RFQ) EPR method [1.4 radicals, cob(II)alamin exchange coupled to a thiyl radical], no cob(II)alamin was observed on the time scale of these experiments (*17*).

For quantitation of cobalamin derivatives, the small molecule products were analyzed assuming a mixture of AdoCbl, HOCbl, and other Co(III) species. Both AdoCbl and HOCbl have $\lambda_{max}$ at 523 nm with an $\varepsilon$ of 8000 $M^{-1}$ $cm^{-1}$. The protein-associated cobalamins were quantitated using GSCbl ($\lambda_{max}$ at 525 nm with an $\varepsilon$ of 8000 $M^{-1}$ $cm^{-1}$), a model for $C_{419}$ attached to the corrin. The spectral features associated with each of these standards are shown in Figure 1S (Supporting Information) The UV−vis spectra of the small molecule products of the inactivation mixture, after concentration, are shown at 2 min and 1 h in panels A and B of Figure 1, respectively. RTPR co-eluted with 0.24 ± 0.3 equiv (average of three experiments) of a cobalt(III)-containing corrin at 2 min and 0.48 ± 0.03 equiv at 1 h. The amount of cob(III)alamin species remaining in solution was 0.65 ± 0.1 and 0.45 ± 0.1 equiv at 2 min and 1 h, respectively. At the 2 min time point, the 0.47 equiv of sugar covalently attached to RTPR and the 0.24 equiv with tightly bound corrin account for the complete inactivation (0.69 equiv). We have shown in our previous pre-steady state studies that recombinant RTPR is only 70−80% active protein (*23*−*26*). As described in more detail subsequently, 0.24 equiv is close to the amount of the $F_2$CTP-derived nucleotide that has been trapped and characterized.

At both 2 min and 1 h, the protein-bound species resembles GSCbl (compare panel A with panel B). More of this material is seen at 1 h, suggesting covalent modification of $C_{419}$ is occurring

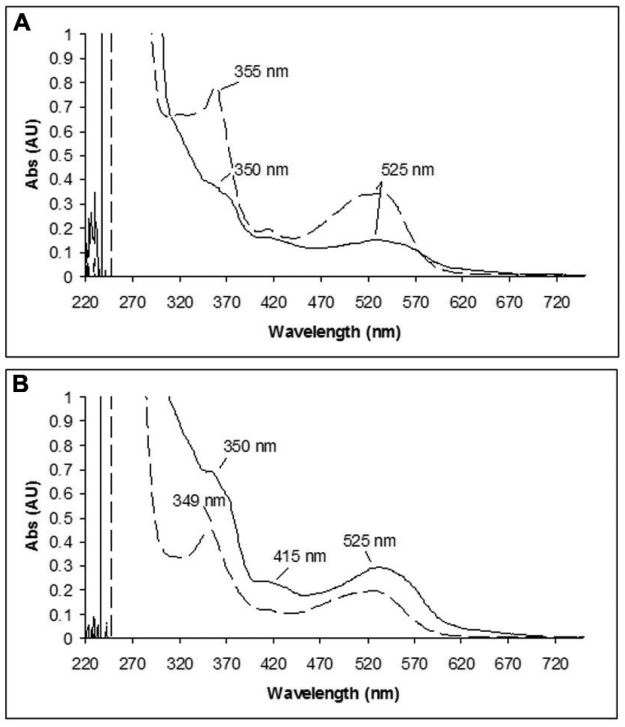


FIGURE 1: UV−vis spectra of the AdoCbl analogue(s) bound to RTPR (—) and in solution (− − −) subsequent to Sephadex G-50 chromatography of RTPR inactivated by $F_2$CTP in the presence of 1 equiv of AdoCbl: (A) after 2 min and (B) after 1 h.

on a slow time scale and continues after complete inactivation (2 min). The spectra of the small molecules are very different at the two time points. Analysis of the 1 h spectrum using linear combinations of AdoCbl and HOCbl showed that a 1:1 (0.2 equiv:0.2 equiv) ratio was able to account for the spectrum (Figure 2S of the Supporting Information). This result is consistent with only 0.8 equiv of AdoCbl being used for complete inactivation. The spectrum for the small molecules observed at 2 min could not be recapitulated by any combination of AdoCbl and HOCbl and at a minimum requires the presence of a third species. While we have obtained a spectrum of this putative third species that appears to be a cobalt(III) species (data not shown), the length of time of the experiment and the concentration of the sample by lyophilization, make any discussion of its structure and whether it is the precursor to RTPR alkylated with a corrin at $C_{419}$ (C419-S corrin) premature.

*Identification and Quantification of the Product(s) Derived from the $F_2$CTP Ribose Ring*. In the following paper (*16*), using 1 equiv of [5-$^3$H]$F_2$CTP, the release of 0.7 equiv of cytosine was found to accompany RTPR inactivation when the reaction mixture was analyzed at 2 min, although the workup took several hours. Furthermore, studies with [1′-$^3$H]$F_2$CTP under identical conditions indicated that 0.47 equiv of sugar was covalently attached to RTPR and that ~0.2 equiv of $F_2$C was recovered. Thus, ~0.3 equiv of the nucleotide is unaccounted for. To find this missing material, inactivations were initially performed using [1′-$^3$H]$F_2$CTP and the small molecules separated from RTPR by ultrafiltration (10 min at 14000*g* and 4 °C) at 2 min. The nucleotides were examined by ion pairing reverse-phase HPLC. The HPLC trace showed new nucleotide products that eluted just prior to $F_2$CTP. These results suggested that there is a nucleotide that has dissociated from RTPR that can eliminate cytosine on a relatively slow time scale. If $F_2$CTP has been converted to

a 3′-ketone as observed for other mechanism-based inhibitors [see Scheme 1 of the following paper (*16*)], it should be possible to reduce it with $NaBH_4$, trapping the product(s) before cytosine and inorganic tripolyphosphate are eliminated.

The inactivation reaction was thus conducted with [1′-$^3$H]$F_2$-CTP for 2 min and then reacted with $NaBH_4$ for 5 min. After the phosphates of the nucleotides were removed with alkaline phosphatase, the reaction mixture was analyzed by reverse-phase HPLC with diode array detection. Under these conditions, in a typical experiment, a small amount of material (< 5%) eluted in the solvent front, 0.25 equiv of $F_2C$ was recovered, and a new, broad peak of radioactivity (0.28 equiv) was observed with a retention time of 17−22 min and a $\lambda_{max}$ at 270 nm, consistent with cytosine-like nucleosides (Figure 2A). The new nucleosides (between the arrow in Figure 2A) were pooled and repurified twice to give a single peak (Figure 2B) with 50% recovery. In each repurification, only the nucleoside with the shorter retention time was pooled. This peak elutes earlier than in the initial purification due to the use of a smaller injection loop (0.5 mL vs 2 mL). There are several reasonable explanations for the heterogeneity of the trapped nucleosides. One explanation is that there was no effort to ensure removal of the borate esters resulting from the reduction process prior to the first chromatography. Repurification and lyophilization in the presence of the $NH_4OAc$ buffer, however, could have catalyzed this hydrolysis and resulted in a more homogeneous sample. A second explanation is that the reduction with $NaBH_4$ of a ketone would produce diastereomers that can be separated by HPLC.

The final product isolated by HPLC was analyzed by NMR spectroscopy and is shown in Figure 3A. The protons at 7.71 and 5.85 ppm are consistent with the H6 and H5 protons of cytosine, respectively, while the proton at 5.99 ppm is consistent with H1′ of a sugar of a nucleoside. An expansion of the sugar ring region from 3.5 to 4.5 ppm (Figure 3A′) showed that the chemical shifts and splitting patterns are similar but not identical to those observed with arabinocytosine (*ara*-C) and cytidine (data not shown). This material has a retention time different from those of cytidine (12.6 min) and *ara*-C (17.4 min), but an ESI-MS spectrum indicates a cytidine isomer. The results together suggest that the nucleoside is an isomer of cytidine differing in stereochemistry at one or more carbons. Selective purification of the nucleoside (Figure 2) is likely to have removed other diastereomers. The trapped nucleoside leads to the surprising conclusion that both fluorines have been eliminated from the $F_2$CTP and an oxygen has been added!

To gain information about the precursor to this cytidine analogue, the inactivation was repeated, using $NaBD_4$ in place of $NaBH_4$ in the quenching process. Our studies with many mechanism-based inhibitors suggested that the radical trapped could be a cytidine derivative with a 3′-ketone and perhaps a radical at C2′ (**6**, Scheme 2) (*3*, *27*−*31*). This radical could rearrange to a 2′-keto 3′- radical through a semidione radical intermediate. Reduction with $NaBD_4$ could then potentially give a mixture of cytidine analogues with $^2$H at C2′ and C3′. HPLC of the reaction mixture revealed that the major trapped nucleoside was similar to that observed by $NaBH_4$ trapping (Figure 2A). The second chromatography of this pooled material is shown in Figure 2C. The third repurification looked like Figure 2B. The material was further purified and characterized by NMR spectroscopy (Figure 3B with an expansion of the sugar region shown in Figure 3B′). The results of this analysis revealed yet another surprise. Greater than 99% $^2$H incorporation was observed at

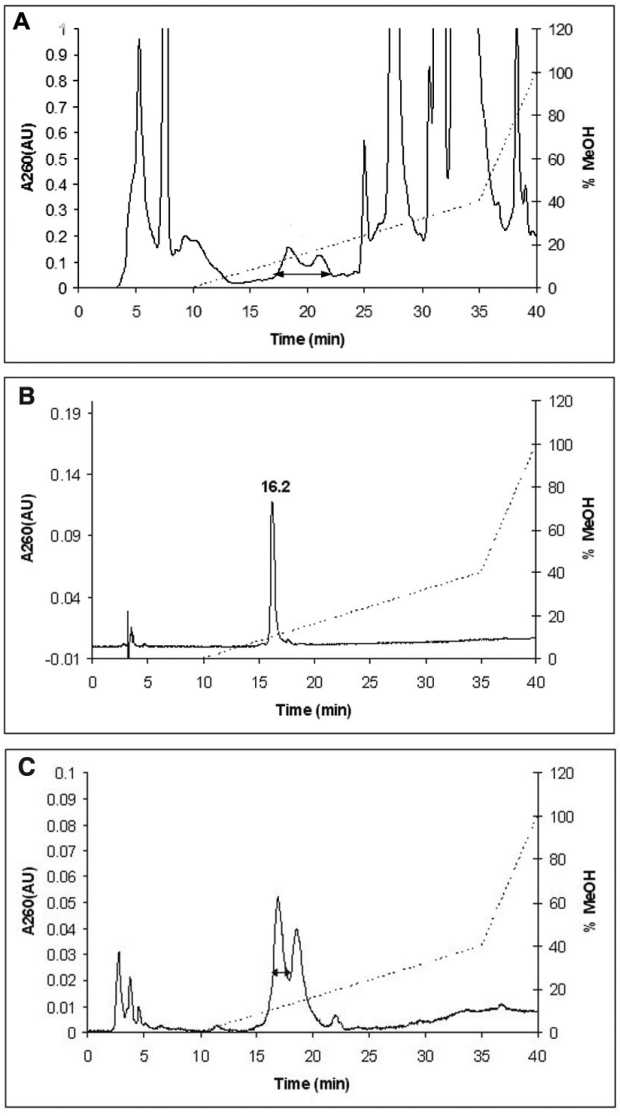


FIGURE 2: Reverse-phase HPLC of small molecules from RTPR inactivated by $F_2$CTP, treated with $NaBH_4$, and dephosphorylated with alkaline phosphatase. $A_{260}$ (—), HPLC gradient (···): buffer A [10 mM $NH_4OAc$ (pH 6.8)] and buffer B (methanol). The double-headed arrow indicates the region pooled in each step. (A) In the initial purification, the material eluting from 17 to 22 min was collected. (B) Elution of the final purified product after two further repurifications under the same conditions. (C) Reverse-phase HPLC of small molecules from RTPR inactivated with $F_2$CTP, treated with $NaBD_4$, and dephosphorylated with alkaline phosphatase. This is the second step in the three-step purification.

both the 2′- and 3′-positions of the nucleoside. The chemical shifts of this trapped material are the same as in the $NaBH_4$-trapped material. The signals, however, for the 2′- and 3′-hydrogens are absent; the signal for the 1′-hydrogen has collapsed to a singlet, and the signal for the 4′-hydrogen has collapsed to a doublet of doublets.

This result requires that the direct precursor to reduction is not a monoketonucleotide as expected, but the 2′,3′-diketonucleotide. This compound would be unable to eliminate cytosine. Thus, the observation of cytosine provides insight into the timing of formation of this material. In the cytosine quantification experiments, it was found that after dephosphorylation of the product mixtures, a process that takes several hours at 37 °C, the only cytosine-containing compounds were cytosine and $F_2C$. Thus, to account for this product, the radical precursor must be oxidized under the $NaBH_4$ quench conditions.

A model for the observed deuterium incorporation is illustrated in Scheme 2. Initial deprotonation of the hydroxyketone radical (**6**) would generate a semidione radical anion (*32*). This compound might undergo reduction by hydride transfer from $NaBH_4$, giving rise **8**. Loss of an electron from **8**, perhaps to $O_2$ or a cobalamin species, would generate a second ketone, which could then be further reduced by $NaBH_4$ to **9**. Reduction of this new ketone would give the observed $^2H$ incorporation. The mechanism of the oxidation process is not known.

*Preliminary Studies Using [1′-$^2$H]$F_2$CTP and [3′-$^2$H]$F_2$CTP and High-Field ENDOR To Probe the Structure of New Radical Species Generated by the Exchange-Coupled Thiyl Radical·Cob(II)alamin: Evidence That This New Species Is Nucleotide-Based.* [1′-$^2$H]$F_2$CTP and [3′-$^2$H]$F_2$CTP were used to investigate the structure of the radical formed upon inactivation of RTPR using X-band (9 GHz) and D-band (130 GHz) EPR methods. Inactivation studies were conducted, and the samples were quenched by hand at 20 or 30 s in an isopentane/liquid $N_2$ slurry. The radical observed with [1′-$^2$H]$F_2$CTP and [3′-$^2$H]$F_2$CTP was identical to the one we previously reported at 9 GHz (data not shown) (*17*). A similar analysis was conducted at high field (130 GHz). No differences were noted between the unlabeled inhibitor and the [3′-$^2$H]$F_2$CTP experiments. With [1′-$^2$H]$F_2$CTP and RTPR, the spectrum was subtly different from that of the unlabeled inhibitor (Figure 3S of the Supporting Information); however, it was unclear whether these differences resulted from deuteration or though interaction with minor radical species. High-frequency ENDOR had a greater potential to show coupling between the deuteron and the radical. The results of these experiments are shown in Figure 4. The spectral regions in which deuteron and proton resonances are expected to be observed are displayed in panels A and B of Figure 4, respectively. At magnetic fields used for D-band ENDOR, the Larmor frequencies of deuterium (31 MHz) and protium (199 MHz) are well-separated and typically provide nonoverlapping spectra. The results of an experiment using [1′-$^2$H]$F_2$CTP are shown in Figure 4A and exhibit 8.6 MHz coupling of the radical to a deuteron. [Note that the quadrupole splitting expected for the deuteron ($I$ = 1) is presumably too small to be resolved in the spectrum.] The corresponding proton coupling in the radical derived from unlabeled $F_2$CTP is evident in Figure 4B (top trace): the peaks at 169 and 226 MHz are split by an amount equal to $(\gamma_H/\gamma_D) \times 8.6$ MHz, in which $\gamma_H$ and $\gamma_D$ are the proton and deuteron gyromagnetic ratios, respectively. This proton coupling is absent in the [1′-$^2$H]$F_2$CTP sample (Figure 4B, bottom). The relative narrowness of both the proton and deuteron peaks together with the insensitivity of the size of the coupling to the excitation position in the EPR spectrum (data not shown) suggests an approximately isotropic hyperfine coupling. In addition, no phosphorus or nitrogen ENDOR couplings were observed (data not shown). These results are consistent with a radical species that has significant unpaired electron spin density at the 2′-position. This unpaired spin density would be expected to couple to the 1′-deuteron/proton via a largely isotropic, $\beta$-hydrogen-type mechanism (*33*, *34*). These preliminary results provided the first direct evidence that the observed organic radical is indeed a nucleotide-based radical and provides support for a mechanism that produces a stable 2′-radical.

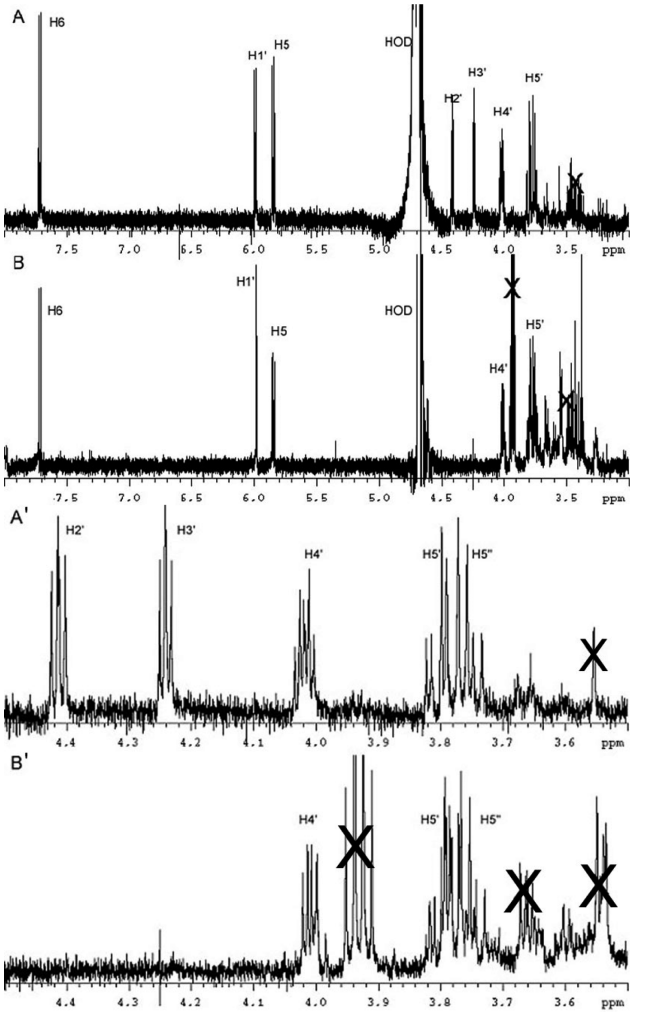


FIGURE 3: Comparison of $^1$H NMR (500 MHz, $D_2O$) spectra of new products isolated from the $NaBH_4$ ($NaB^2H_4$) quench of RTPR inactivated with $F_2$CTP: (A) product from the $NaBH_4$ quench and (B) product from the $NaB^2H_4$ quench. (A′ and B′ are expansions of spectra A and B, respectively, in the region from 3.5 to 4.5 ppm). The nucleoside proton resonances are labeled. Several impurity peaks can be seen; these are marked with an X. Further, the H5−H5′ region in spectrum B appears to overlap with an impurity peak.

## DISCUSSION

A nonalkylative pathway required for complete inactivation of RTPR by $F_2$CTP involves reaction of the enzyme with the AdoCbl, ultimately resulting in the formation of a bond between the Co in the corrin and S of $C_{419}$ that we have previously characterized (*17*). Our studies that examined the fate of AdoCbl

Scheme 2: Proposed Mechanism for Incorporation of Deuterium into the Nucleotide Trapped by $NaB^2H_4$ Subsequent to the Inactivation of RTPR by $F_2$CTP

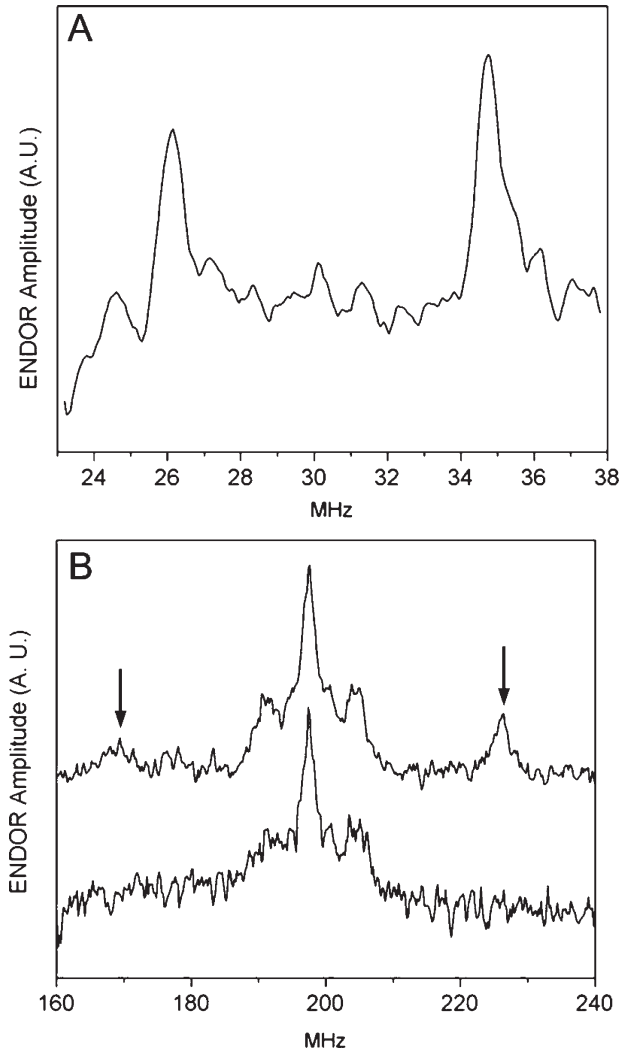


FIGURE 4: High-frequency (130 GHz) Davies ENDOR of $F_2$CTP reacted with RTPR for 30 s. (A) Deuterium ENDOR of the [1′-$^2$H]$F_2$-CTP reaction: temperature of 7 K; 8000 averages per point; pulse widths of 80, 40, and 80 ns; RF pulse width of 20 $\mu$s; tau of 200 ns; repetition rate of 100 Hz. (B) Proton ENDOR: temperature of 7 K; pulse widths of 70, 35, and 70 ns; RF pulse width of 6.8 $\mu$s; tau of 200 ns; repetition rate of 100 Hz. The top trace shows data for RTPR reacted with [1′-$^1$H]$F_2$CTP (800 averages per point). The peaks at 169 and 226 MHz are indicated. The bottom trace shows data for RTPR reacted with [1′-$^2$H]$F_2$CTP (4500 averages per point).

reveal that after 2 min, 0.25 equiv of the cobalt(III) species co-elutes with RTPR and displays a spectrum consistent with a corrin containing a Co−S bond (compare Figure 1A with Figure 1S). By 1 h, the amount of this species (Figure 1B) has increased to 0.45 equiv, with a corresponding decrease in the anount of the corrin species in solution. The unidentified Co(III) species present in the small molecules at 2 min disappears by 1 h, suggesting it is converted into the Co−S adduct. Thus, 100% inactivation is associated with a tightly bound AdoCbl analogue in the +3 oxidation state, which is slowly converted into the previously characterized Co−S adduct.

In addition to this tightly bound corrin associated with RTPR at 2 min, 0.25 equiv of a nucleotide derived from $F_2$CTP was trapped with $NaBH_4$ in which both fluorines were lost and a water molecule was added. As argued subsequently, our hypothesis is that this trapped nucleotide is derived from radical **4** in Scheme 1. While the identity of **4** has not been unambiguously established, the HFEPR/HFENDOR data presented are consistent with a 3′-keto, 2′-oxoallylic radical species such as **4**. The largely isotropic 1′-$^1$H and $^2$H couplings of 57 and 8.6 MHz, respectively, are in agreement with calculations published previously for such a radical species (*35*). In addition, the splitting in the proton spectra of approximately 13 MHz (Figure 4B) is consistent with calculations for the proton at the 4′-position (*35*). From the EPR data, there is no evidence of the presence of fluorine, consistent with **4**.

Our working hypothesis that accounts for the nonalkylative pathway and formation of **4** is shown in Scheme 1. Our previous RFQ EPR experiments during the inactivation of RTPR by $F_2$CTP revealed that a thiyl radical exchange coupled to cob(II)alamin (1.4 equiv of radical) was present within 20 ms, the first time point. This radical pair gave rise quantitatively to a new radical pair over 220 ms that is proposed to be **2**↔**3** and cob(II)alamin (Scheme 1). Formation of **2**↔**3** is proposed to occur, by loss of $F^-$ without protonation by the proximal bottom-face cysteine, $C_{119}$. The loss of $F^-$ and not HF might result if the ribose ring of the nucleotide is too far removed from $C_{119}$, as suggested by the recent crystal structure of the *Saccharomyces cerevisiae* RNR (*36*). Alternatively, $F^-$ loss may simply be related to its leaving group ability being intermediate between those of hydroxide, which with the normal substrate must be protonated to leave at a reasonable rate, and chloride, which can be lost without protonation (*37*). Radical **2**↔**3**, the species we believe was detected at 220 ms by RFQ experiments, could then react with water at C2′, in a reaction that is the reversal of water elimination in the normal reaction (considered irreversible for the normal, nonfluorinated substrate). In the nonalkylative pathway, **3** could now eliminate the second $F^-$, generating **4**, the favored structure for the stable radical seen at 20 s (*17*). This radical is structurally very similar to the stable glycoaldehyde radical detected when diol dehydratase is inactivated by glycoaldehyde (*32*, *38*). The glycoaldehyde radical is reported to be stable for days at room temperature under anaerobic conditions. Radical **4** could dissociate from the active site and eventually decompose to eliminate cytosine or be trapped if $NaBH_4$ is present, prior to cytosine release. In the alkylative pathway (from **3** to **5**, Scheme 1), we propose that protonation of $F^-$ occurs by $C_{119}$, giving loss of HF. The resulting thiolate of $C_{119}$ could now attack the C2′ atom of the nucleotide to form the alkylated protein.

The model of inactivation of RTPR by $F_2$CTP is complex but shares many common features with inactivation of the class Ia RNRs (*Escherichia coli* and the two human RNRs) despite the differences in the cofactor requirement (*39*−*41*). In each enzyme, the inactivation is stoichiometric and involves multiple pathways: alkylation of an active site cysteine and destruction of the cofactor (AdoCbl or Y$^\bullet$). The alkylation is accompanied by a change in conformation of the RNR large subunit (α) that can be observed by SDS−PAGE analysis if the sample is not boiled prior to being loaded on the gel. The conformational change results in an α that migrates more slowly than unmodified α (*41*). In both the case of the *E. coli* RNR and the *L. leichmannii* RNR, a new nucleotide radical is generated, resulting in the destruction of the cofactor (*41*). In both cases, we propose that the structure of the radical is the same, resulting from the loss of two fluorines and addition of a water molecule. The major distinction between $F_2$C nucleotides and previously studied 2′-substituted 2′-deoxynucleotides is the presence of the second leaving group. As with many fluorinated mechanism-based inhibitors, the presence of the second fluoride causes the reaction to be irreversible (*42*).

The similarities between the chemistry of the class I and II RNRs suggest that lessons learned from our studies on inactivation of the *L. leichmannii* RTPR will likely be very informative with respect to the mechanisms of inactivation of the class Ia RNRs by this clinically useful antitumor agent.

## SUPPORTING INFORMATION AVAILABLE

UV−vis spectra of cobalamin standards (Figure 1S) and small molecule fraction from Sephadex G-50 chromatography of the inactivation experiment (Figure 2S) and 130 GHz EPR spectra of RTPR with $F_2$CTP and [1′-$^2$H]$F_2$CTP (Figure 3S). This material is available free of charge via the Internet at http://pubs.acs.org.

## REFERENCES


1. Stubbe, J., and van der Donk, W. A. (1995) Ribonucleotide reductases: Radical enzymes with suicidal tendencies. *Chem. Biol. 2*, 793–801.
2. Stubbe, J., and van der Donk, W. A. (1998) Protein radicals in enzyme catalysis. *Chem. Rev. 98*, 705–762.
3. Licht, S., and Stubbe, J. (1999) Mechanistic investigations of ribonucleotide reductases. In Comprehensive Natural Products Chemistry (Barton, S. D., Nakanishi, K., Meth-Cohn, O., and Poulter, C. D., Eds.) pp 163−203, Elsevier Science, New York.
4. Eklund, H., Uhlin, U., Färnegardh, M., Logan, D. T., and Nordlund, P. (2001) Structure and function of the radical enzyme ribonucleotide reductase. *Prog. Biophys. Mol. Biol. 77*, 177–268.
5. Nordlund, P., and Reichard, P. (2006) Ribonucleotide reductases. *Annu. Rev. Biochem. 75*, 681–706.
6. Hertel, L. W., Boder, G. B., Kroin, J. S., Rinzel, S. M., Poore, G. A., Todd, G. C., and Grindley, G. B. (1990) Evaluation of the antitumor activity of gemcitabine (2′,2′-difluoro-2′-deoxycytidine). *Cancer Res. 51*, 6110–6117.
7. Hertel, L. W., Kroin, J. S., Grossman, C. S., Grindey, G. B., Door, A. F., Storinolo, A. M. V., Plunkett, W., Gandhi, V., and Huang, P. (1996) Synthesis and biological activity of 2′,2′-difluorodeoxycytidine (gemcitabine). In Biomedical Frontiers of Fluorine Chemistry (Ojima, I., McCarthy, J. R., and Welch, J. T., Eds.) American Chemical Society, Washington, DC.
8. Huang, P., Chubb, S., Hertel, L. W., Grindey, G. B., and Plunkett, W. (1991) Action of 2′,2′-difluorodeoxycytidine on DNA synthesis. *Cancer Res. 51*, 6110–6117.
9. Davidson, J. D., Ma, L., Flagella, M., Geeganage, S., Gelbert, L. M., and Slapak, C. A. (2004) An increase in the expression of ribonucleotide reductase large subunit 1 is associated with gemcitabine resistance in non-small cell lung cancer cell lines. *Cancer Res. 64*, 3761–3766.
10. Danesi, R., Altavilla, G., Giovannetti, E., and Rosell, R. (2009) Pharmacogenetics of gemcitabine in non-small-cell lung cancer and other solid tumors. *Pharmacogenetics 10*, 69–80.
11. Rivera, F., López-Tarruella, S., Vega-Villegas, M. E., and Salcedo, M. (2009) Treatment of advanced pancreatic cancer: From gemcitabine single agent to combinations and targeted therapy. *Cancer Treat. Rev. 35*, 335–339.
12. Jordan, A., Torrents, E., Jeanthon, C., Eliasson, R., Hellman, U., Wernstedt, C., Barbé, J., Gibert, I., and Reichard, P. (1997) $B_{12}$-dependent ribonucleotide reductases from deeply rooted eubacteria are structurally related to the aerobic enzyme from *Escherichia coli*. *Proc. Natl. Acad. Sci. U.S.A. 94*, 13487–13492.
13. Booker, S., and Stubbe, J. (1993) Cloning, sequencing and expression of the adenosylcobalamin-dependent ribonucleotide reductase from *Lactobacillus leichmannii*. *Proc. Natl. Acad. Sci. U.S.A. 90*, 8352–8356.
14. Sintchak, M. D., Arjara, G., Kellogg, B. A., Stubbe, J., and Drennan, C. L. (2002) The crystal structure of class II ribonucleotide reductase reveals how an allosterically regulated monomer mimics a dimer. *Nat. Struct. Biol. 9*, 293–300.
15. Larsson, K.-M., Jordan, A., Eliasson, R., Reichard, P., Logan, D. T., and Nordlund, P. (2004) Structural mechanism of allosteric substrate specificity regulation in a ribonucleotide reductase. *Nat. Struct. Mol. Biol. 11*, 1142–1149.
16. Lohman, G. J. S., and Stubbe, J. (2010) Inactivation of *Lactobacillus leichmannii* ribonucleotide reductase by $F_2$CTP: Covalent modification. *Biochemistry 49*, DOI: 10.1021/bi902132u.
17. Silva, D. J., Stubbe, J., Samano, V., and Robins, M. J. (1998) Gemcitabine 5′-triphosphate is a stoichiometric mechanism-based inhibitor of *Lactobacillus leichmannii* ribonucleoside triphosphate reductase: Evidence for thiyl radical-mediated nucleotide radical formation. *Biochemistry 37*, 5528–5535.
18. Stubbe, J., and Riggs-Gelasco, P. (1998) Harnessing free radicals: Formation and function of the tyrosyl radical in ribonucleotide reductase. *Trends Biochem. Sci. 23*, 438–443.
19. Bandarian, V., Ludwig, M. L., and Matthews, R. G. (2003) Factors modulating conformational equilibria in large modular proteins: A case study with cobalamin-dependent methionine synthase. *Proc. Natl. Acad. Sci. U.S.A. 100*, 8156–8163.
20. Krymov, V., and Gerfen, G. J. (2003) Analysis of the tuning and operation of reflection resonator EPR spectrometers. *J. Magn. Reson. 162*, 466–478.
21. Ranguelova, K., Girotto, S., Gerfen, G. J., Yu, S., Suarez, J., Metlitsky, L., and Magliozzo, R. S. (2007) Analysis of the tuning and operation of reflection resonator EPR spectrometers. *J. Biol. Chem. 282*, 6255–6264.
22. Burhaus, O., Rohrer, M., Plato, M., and Mobius, K. (1992) A novel high-field/high frequency EPR and ENDOR spectrometer operating at 3 mm wavelength. *Meas. Sci. Technol. 3*, 765–774.
23. Booker, S., Licht, S., Broderick, J., and Stubbe, J. (1994) Coenzyme $B_{12}$-dependent ribonucleotide reductase: Evidence for the participation of five cysteine residues in ribonucleotide reduction. *Biochemistry 33*, 12676–12685.
24. Licht, S. S., Booker, S., and Stubbe, J. (1999) Studies on the catalysis of carbon-cobalt bond homolysis by ribonucleoside triphosphate reductase: Evidence for concerted carbon-cobalt bond homolysis and thiyl radical formation. *Biochemistry 38*, 1221–1233.
25. Licht, S. S., Lawrence, C. C., and Stubbe, J. (1999) Thermodynamic and kinetic studies on carbon-cobalt bond homolysis by ribonucleoside triphosphate reductase: The importance of entropy in catalysis. *Biochemistry 38*, 1234–1242.
26. Licht, S. S., Lawrence, C. C., and Stubbe, J. (1999) Class II ribonucleotide reductases catalyze carbon-cobalt bond reformation on every turnover. *J. Am. Chem. Soc. 121*, 7463–7468.
27. Ator, M. A., and Stubbe, J. (1985) Mechanism of inactivation of *Escherichia coli* ribonucleotide reductase by 2′-chloro-2′-deoxyuridine 5′-diphosphate: Evidence for generation of 2′-deoxy-3′-ketonucleotide via a net 1,2 hydrogen shift. *Biochemistry 24*, 7214–7221.
28. Harris, G., Ator, M., and Stubbe, J. (1984) Mechanism of inactivation of *Escherichia coli* and *Lactobacillus leichmannii* ribonucleotide reductases by 2′-chloro-2′-deoxynucleotides: Evidence for generation of 2-methylene-3(2*H*)-furanone. *Biochemistry 23*, 5214–5225.
29. van der Donk, W. A., Stubbe, J., Gerfen, G. G., Bellew, B. F., and Griffin, R. G. (1995) EPR investigations of the inactivation of *E. coli* ribonucleotide reductase with 2′-azido-2′-deoxyuridine 5′-diphosphate: Evidence for the involvement of the thiyl radical of C225-R1. *J. Am. Chem. Soc. 117*, 8909–8916.
30. van der Donk, W. A., Yu, G., Pérez, L., Sanchez, R. J., and Stubbe, J. (1998) Detection of a new substrate-derived radical during inactivation of ribonucleotide reductase from *Escherichia coli* by gemcitabine 5′-diphosphate. *Biochemistry 37*, 6419–6426.
31. Gerfen, G. G., van der Donk, W. A., Yu, G., McCarthy, J. R., Jarvi, E. T., Matthews, D. P., Farrar, C., Griffin, R. G., and Stubbe, J. (1998) Characterization of a substrate-derived radical detected during the inactivation of ribonucleotide reductase from *Escherichia coli* by 2′-fluoromethylene-2′-deoxycytidine 5′-diphosphate. *J. Am. Chem. Soc. 120*, 3823–3835.
32. Sandala, G. M., Smith, D. M., Coote, M. L., Golding, B. T., and Radom, L. (2006) Insights into the hydrogen-abstraction reactions of diol dehydratase: Relevance to the catalytic mechanism and suicide inactivation. *J. Am. Chem. Soc. 128*, 3433–3444.
33. Heller, C., and McConnell, H. M. (1960) Radiation Damage in Organic Crystals. II. Electron Spin Resonance of $(CO_2H)CH_2$-$CH(CO_2H)$ in $\beta$-Succinic Acid. *J. Chem. Phys. 32*, 1535–1539.
34. Derbyshire, W. (1962) The coupling between an unpaired electron spin and a proton two bonds away. *Mol. Phys. 5*, 225–231.
35. Zipse, H., Artin, E., Wnuk, S., Lohman, G. J., Martino, D., Griffin, R. G., Kacprzak, S., Kaupp, M., Hoffman, B., Bennati, M., Stubbe, J., and Lees, N. (2009) Structure of the nucleotide radical formed during reaction of CDP/TTP with the E441Q-$\alpha 2\beta 2$ of *E. coli* ribonucleotide reductase. *J. Am. Chem. Soc. 131*, 200–211.
36. Xu, H., Faber, C., Uchiki, T., Racca, J., and Dealwis, C. (2006) Structures of eukaryotic ribonucleotide reductase I define gemcitabine diphosphate binding and subunit assembly. *Proc. Natl. Acad. Sci. U.S.A. 103*, 4028–4033.
37. Harris, G., Ashley, G. W., Robins, M. J., Tolman, R. L., and Stubbe, J. (1987) 2′-Deoxy-2′-halonucleotides as alternate substrates and

mechanism-based inactivators of *Lactobacillus leichmannii* ribonucleotide reductase. *Biochemistry 26*, 1895–1902.
38. Abend, A., Bandarian, V., Reed, G. H., and Frey, P. A. (2000) Identification of *cis*-ethanesemidione as the organic radical derived from glycolaldehyde in the suicide inactivation of dioldehydrase and of ethanolamine ammonia-lyase. *Biochemistry 39*, 6250–6257.
39. Wang, J., Lohman, G. J., and Stubbe, J. (2007) Enhanced subunit interactions with gemcitabine-5′-diphosphate inhibit ribonucleotide reductases. *Proc. Natl. Acad. Sci. U.S.A. 104*, 14324–14329.
40. Wang, J., Lohman, G. J., and Stubbe, J. (2009) Mechanism of inactivation of human ribonucleotide reductase with p53R2 by gemcitabine-5′-diphosphate. *Biochemistry 48*, 11612–11621.
41. Artin, E., Wang, J., Lohman, G. J. S., Yu, G., Griffin, R. G., Barr, G., and Stubbe, J. (2009) Insight into the mechanism of inactivation of ribonucleotide reductase by gemcitabine 5′-diphosphate in the presence and absence of reductant. *Biochemistry 48*, 11622–11629.
42. Walsh, C. T. (1983) Fluorinated substrate analogs: Routes of metabolism and selective toxicity. *Adv. Enzymol. Relat. Areas Mol. Biol. 55*, 197–289.